Manuscript

Higher mortality rates leave heated ecosystem with similar size-structure despite larger, younger, and faster growing fish

Max Lindmark[a,1], Malin Karlsson[a], Anna Gårdmark[b]

[a] Swedish University of Agricultural Sciences, Department of Aquatic Resources, Institute of Coastal Research, Skolgatan 6, 742 42 Öregrund, Sweden

[b] Swedish University of Agricultural Sciences, Department of Aquatic Resources, Box 7018, 750 07 Uppsala, Sweden

[1] Author to whom correspondence should be addressed. Current address:
Max Lindmark, Swedish University of Agricultural Sciences, Department of Aquatic Resources, Institute of Marine Research, Turistgatan 5, 453 30 Lysekil, Sweden, Tel.: +46(0)104784137, email: max.lindmark@slu.se

Keywords: body growth, size-structure, size-spectrum, mortality, climate change, global warming, temperature

Abstract

Ectotherms are often predicted to "shrink" with global warming, in line with general growth models and the temperature-size rule (TSR), both predicting smaller adult sizes with warming.

However, they also predict faster juvenile growth rates, leading to larger size-at-age. Hence, the result of warming on the size-structure of a population depends on the interplay between how mortality rate, juvenile- and adult growth rates are affected by warming. In this study, we use time series of biological samples spanning more than two decades from a unique enclosed bay heated by cooling water from a nearby nuclear power plant to become +8C warmer than its reference area. We used growth-increment biochronologies (12658 reconstructed length-at-age estimates) to quantify how the >20 years of warming has affected body growth and size-at-age and catch data to quantify mortality rates and population size-structure of Eurasian perch (*Perca fluviatilis*). In the heated area, growth rates were higher for all sizes, and hence size-at-age was larger for all ages, compared to the reference area. However, mortality rates were also higher, such that the difference in the size-spectrum exponent (describing the proportion of fish by size) was relatively minor and statistically uncertain. As such, our analysis reveals that mortality, in addition to plastic growth and size-responses, is a key factor determining the size structure of populations exposed to warming. Understanding the mechanisms by which warming affects the size-structure of populations is critical for prediction the impacts of climate change on ecological functions, interactions, and dynamics.

Significance statement

Ecosystem-scale warming experiments provide unique insight into potential impacts of climate change but are very rare. Our work utilizes an experimental set-up consisting of an enclosed

bay heated by cooling water from a nuclear power plant for more than two decades, and a reference area. We analyze how changes in growth and mortality have affected the size- and age distribution in a common freshwater fish using time series of catch data and growth-increment biochronologies derived from their gill lids. Despite fish in the heated area being ~10% larger at a given age, elevated mortality rates have caused similar size structures. Accounting for the interplay between mortality and growth is key for predictions of climate impacts on the size-structure of populations.

Introduction

Ectotherm species, constituting 99% of species globally(1, 2), are commonly predicted to shrink in a warming world(3–5). Mean body size responses to temperature may however be

uninformative, as the size-distribution of many species spans several orders of magnitude. For instance, warming can shift size-distributions without altering mean size if increases in juvenile size-at-age outweigh the decline in size-at-age in adults, which is consistent with the temperature size-rule, TSR(6). Resolving how warming induces changes in population size-distributions may thus be more instructive(7), especially for inferring warming effects on species' ecological role, biomass production, or energy fluxes(8). This is because key processes such as metabolism, feeding, growth, mortality scale with body size(9–14). Hence, as the value of these traits at mean body size is not the same as the mean population trait value(15), the size-distribution within a population matters for its dynamics and for how it changes under warming.

The population size distribution can be represented as a size-spectrum, which generally is the frequency distribution of individual body sizes(16). It is often described in terms of the size-spectrum slope (slope of individuals or biomass of a size class over the mean size of that class on log-log scale(16–18)) or simply the exponent of the power law individual size-distribution(16). The size-spectrum thus results from temperature-dependent ecological processes such as body growth, mortality and recruitment(10, 19). Despite its rich theoretical foundation(20) and usefulness as an ecological indicator(21), few studies have evaluated warming-effects on the species size-spectrum in larger bodied species (but see Blanchard *et al.*(21)), and none in large scale experimental set-ups. There are numerous paths by which the species size-spectrum could change with warming(19). For instance, in line with TSR predictions, warming may lead to a smaller size-spectrum exponents (steeper slope) if the maximum size. However, changes in size-at-age and the relative abundances of juveniles and adults may alter this decline in the size-spectrum slope. Warming can also lead to elevated mortality(12, 22–24), which truncates the age-distribution towards younger individuals(25). This may reduce density dependence and potentially increase growth rates, thus countering the

100 effects of mortality on the size spectrum exponent. However, this depends on which sizes
101 benefit from warming (26, 27). Hence, the effect of warming on the size-spectrum depends on
102 several interlinked processes affecting abundance-at-size and size-at-age.
103 Size-at-age is generally predicted to increase with warming for small individuals, but
104 decrease for large individuals (according to the mentioned TSR(6, 28)). Several factors likely
105 contribute to this pattern, such as increased allocation to reproduction (29) and larger
106 individuals in fish populations reaching optimum growth rates at lower temperatures(27).
107 Empirical support in fishes for this pattern seem to be more consistent for increases in size-at-
108 age of juveniles(30–32) than declines in adult size-at-age (but see (33–35)), for which a larger
109 diversity in responses is observed among species(32, 36). In addition, most studies have been
110 done on commercially exploited species (since long time series are more common in such
111 species). However, size- and growth trends over time may also be affected by plastic and/or
112 genetic responses to size-selective mortality(37). Moreover, the effect of temperature on
113 mortality rates of wild populations are more studied using among-species analyses. These
114 relationships based on thermal gradients in space may not necessarily be the same as the effects
115 of *warming* on mortality on single populations. Hence, the effects of warming on growth and
116 size-at-age and mortality within natural populations constitute a key knowledge gap for
117 predicting the consequences of climate change on population size-spectra.
118 Here we used data from a unique, large-scale 23-year-long heating-experiment of a coastal
119 ecosystem to quantify how warming changed fish body growth, mortality, and the size structure
120 in an unexploited population of Eurasian perch (*Perca fluviatilis*, 'perch'). We compare fish
121 from this enclosed bay exposed to temperatures approximately 8℃ above normal ('heated
122 area') with fish from a reference area in the adjacent archipelago (Fig. 1). Using hierarchical
123 Bayesian models, we quantify differences in key individual- and population level parameters,

such as body growth, asymptotic size, mortality rates, and size-spectra, between the heated and reference coastal area.

Materials and Methods

Data

We use size-at-age data from perch sampled annually from an artificially heated enclosed bay ('the Biotest basin') in the western Baltic Sea and its reference area (Fig. 1) with natural temperatures in the years after the onset of warming. Heating started in 1980, the first analyzed cohort is 1981, and first and last catch year is 1987 and 2003, respectively, to omit transient dynamics and acute responses, and to ensure we use cohorts that only experienced one of the thermal environments during its life. A grid at the outlet of the heated area (Fig. 1) prevented fish larger than 10 cm from migrating between the areas(32, 38), and genetic studies confirm the reproductive isolation between the two populations during this time-period(39). However, since the grid removal in 2004, fish growing up in the heated Biotest basin can easily swim out, meaning we cannot be sure fish in the reference area did not recently arrive from the Biotest basin. Hence, we use data only up until 2003. This resulted in 12658 length-at-age measurements from 2426 individuals in 256 net deployments.

We use data from fishing events using survey-gillnets that took place in October in the heated Biotest basin and in August in the reference area when temperatures are most comparable between the two areas(32), because temperature affect catchability in static gears. The catch was recorded by 2.5 cm length classes during 1987-2000, and into 1 cm length groups 2001-2003. To express lengths in a common length standard, 1 cm intervals were converted into 2.5 cm intervals. The unit of catch data is hence the number of fish caught per 2.5 cm size class per net per night (i.e., a catch-per-unit-effort [CPUE] variable). All data from fishing events with disturbance affecting the catch (e.g., seal damage, strong algal growth on the gears,

clogging by drifting algae) were removed (years 1996 and 1999 from the heated area in the catch data).

Length-at-age throughout life was reconstructed for a semi-random length-stratified subset of caught individuals each year. This was done using growth-increment biochronologies derived from annuli rings on the operculum bones (with control counts done on otoliths). Such analyses have become increasingly used to analyze changes in growth and size-at-age of fishes(40, 41). Specifically, we used an established power-law relationship between the distance of annual rings and fish length: $L = \kappa R^s$, where L is the length of the fish, R the operculum radius, κ the intercept, and s the slope of the line for the regression of log-fish length on log-operculum radius from a large reference data set for perch(42). Back-calculated length-at-age were obtained from the relationship $L_a = L_s(\frac{r_a}{R})^s$, where L_a is the back-calculated body length at age a, L_s is the final body length (body length at catch), r_a is the distance from the center to the annual ring corresponding to age a and $s = 0.861$ for perch(42). Since perch exhibits sexual size-dimorphism, and age-determination together with back calculation of growth was not done for males in all years, we only used females for our analyses.

Statistical Analysis

The differences in size-at-age, growth, mortality, and size structure between perch in the heated and the reference area were quantified using hierarchical linear and non-linear regression models fitted in a Bayesian framework. First, we describe each statistical model and then provide details of model fitting, model diagnostics and comparison.

We fit the von Bertalanffy growth equation (VBGE)(43, 44) on a log scale, describing length as a function of age to evaluate differences in size-at-age and asymptotic size: $\log(L_t) = \log(L_\infty(1 - e^{(-K(t-t_0))}))$, where L_t is the length at age (t, years), L_∞ is the asymptotic size,

K is the Brody coefficient (yr^{-1}) and t_0 is the age when the average length was zero. We used only age- and size-at-catch as the response variables (i.e., not back-calculated length-at-age). This was to have a simpler model and not have to account for parameters varying within individuals as well as cohorts, as mean sample size per individual was only ~5. We let parameters vary among cohorts rather than year of catch, because individuals within cohorts share similar environmental conditions and density dependence(40). Eight models in total were fitted (with area being dummy-coded), with different combinations of shared and area-specific parameters. We evaluated if models with area-specific parameters led to better fit and quantified the differences in area-specific parameters (indexed by subscripts heat and ref). The model with all area-specific parameter can be written as:

$$L_i \sim \text{Student-}t(\upsilon, \mu_i, \sigma) \tag{1}$$

$$\log(\mu_i) = A_{ref} \log\left[L_{\infty ref j[i]}\left(1 - e^{\left(-K_{ref j[i]}\left(t - t_{0 ref j[i]}\right)\right)}\right)\right] + A_{heat} \log\left[L_{\infty heat j[i]}\left(1 - e^{\left(-K_{heat j[i]}\left(t - t_{0 heat j[i]}\right)\right)}\right)\right] \tag{2}$$

$$\begin{bmatrix} L_{\infty ref j} \\ L_{\infty heat j} \\ K_{ref j} \\ K_{heat j} \end{bmatrix} \sim \text{MVNormal}\left(\begin{bmatrix} \mu_{L_{\infty ref}} \\ \mu_{L_{\infty heat}} \\ \mu_{K_{ref}} \\ \mu_{K_{heat}} \end{bmatrix}, \begin{bmatrix} \sigma_{L_{\infty ref}} & 0 & 0 & 0 \\ 0 & \sigma_{L_{\infty heat}} & 0 & 0 \\ 0 & 0 & \sigma_{K_{ref}} & 0 \\ 0 & 0 & 0 & \sigma_{K_{heat}} \end{bmatrix}\right) \tag{3}$$

where lengths are $Student - t$ distributed to account for extreme observations, υ, μ and ϕ represent the degrees of freedom, mean and the scale parameter, respectively. A_{ref} and A_{heat} are dummy variables such that $A_{ref} = 1$ and $A_{heat} = 0$ if it is the reference area, and vice versa for the heated area. The multivariate normal distribution in Eq. 3 is the prior for the cohort-varying parameters $L_{\infty ref j}$, $L_{\infty heat j}$, $K_{ref j}$ and $K_{heat j}$ (for cohorts $j = 1981,\ldots,1997$) (note that cohorts extend further back in time than the catch data), with hyper-parameters $\mu_{L_{\infty ref}}$, $\mu_{L_{\infty heat}}$, $\mu_{K_{ref}}$, $\mu_{K_{heat}}$ describing the non-varying population means and a covariance matrix with the between-cohort variation along the diagonal (note we did not model a correlation between the parameters, hence off-diagonals are 0). The other seven models include

some or all parameters as parameters common for the two areas, e.g., substituting $L_{\infty ref j}$ and $L_{\infty heat j}$ with $L_{\infty j}$. To aid convergence of this non-linear model, we used informative priors chosen after visualizing draws from prior predictive distributions(45) using probable parameter values (*Supporting Information*, Fig. S1, S7). We used the same prior distribution for each parameter class for both areas to not introduce any other sources of differences in parameter estimates between areas. We used the following priors for the VBGE model: $\mu_{L_{\infty ref,heat}} \sim N(45,20)$, $\mu_{K_{ref,heat}} \sim N(0.2, 0.1)$, $t_{0ref,heat} \sim N(-0.5, 1)$ and $\upsilon \sim gamma(2,0.1)$. $\sigma, \mu_{L_{\infty ref}}, \mu_{L_{\infty heat}}, \mu_{K_{ref}}, \mu_{K_{heat}}$ were given a $Student - t(3,0,2.5)$ prior.

We also compared how body growth scales with body size (in contrast to length vs age). This is because size-at-age reflects lifetime growth history rather than current growth histories and may thus be large because growth was fast early in life, not because current growth rates are fast(46). We therefore fit allometric growth models describing how specific growth rate scales with length: $G = \alpha L^{\theta}$, where G, the annual specific growth between year t and $t+1$, is defined as: $G = 100 \times (log\,(L_{t+1}) - log\,(L_t))$ and L is the geometric mean length: $L = (L_{t+1} \times L_t)^{0.5}$. Here we also used back-calculated length-at-age, resulting in multiple observations for each individual. As with the VBGE model, we dummy coded area to compare models with different combinations of common and shared parameters. We assumed growth rates were $Student - t$ distributed, and the full model can be written as:

$$L_i \sim Student - t(\upsilon, \mu_i, \sigma) \quad (4)$$

$$\mu_i = A_{ref}\left(\alpha_{ref j[i],k[i]} L^{\theta_{ref}}\right) + A_{heat}\left(\alpha_{heat j[i],k[i]} L^{\theta_{heat}}\right) \quad (5)$$

$$\alpha_{ref,heat j} \sim N\left(\mu_{\alpha_{ref,heat j}}, \sigma_{\alpha_{ref,heat j}}\right) \quad (6)$$

$$\alpha_{ref,heat j} \sim N\left(\mu_{\alpha_{ref,heat j}}, \sigma_{\alpha_{ref,heat j}}\right) \quad (7)$$

$$\theta_{ref,heat j} \sim N\left(\mu_{\theta_{ref,heat j}}, \sigma_{\theta_{ref,heat j}}\right) \quad (8)$$

$$\theta_{ref,heat j} \sim N\left(\mu_{\theta_{ref,heat j}}, \sigma_{\theta_{ref,heat j}}\right) \quad (9)$$

We assumed only α varied across individuals j within cohorts k and compared two models: one with θ common for the heated and reference area, and one with an area-specific θ. We

used the following priors, after visual exploration of the prior predictive distribution (*Supporting Information*, Fig. S8, S10): $\alpha_{ref,heat} \sim N(500, 100)$, $\theta_{ref,heat} \sim N(-1.2, 0.3)$ and $v \sim gamma(2, 0.1)$. σ, $\sigma_{id:cohort}$ and σ_{cohort} were all given a $Student - t(3, 0, 13.3)$ prior.

We estimated total mortality by fitting linear models to the natural log of catch (CPUE) as a function of age (catch curve regression), under the assumption that in a closed population, the exponential decline can be described as $N_t = N_0 e^{-Zt}$, where N_t is the population at time t, N_0 is the initial population size and Z is the instantaneous mortality rate. This equation can be rewritten as a linear equation: $log\ (C_t) = log\ (vN_0) - Zt$, where C_t is catch at age t, if catch is assumed proportional to the number of fish (i.e., $C_t = vN_t$). Hence, the negative of the slope of the regression is the mortality rate, Z. To get catch-at-age data, we constructed area-specific age-length keys using the sub-sample of the total (female) catch that was age-determined. Age length-keys describe the age-proportions of each length-category (i.e., a matrix with length category as rows, ages as columns). Age composition is then estimated for the total catch based on the "probability" of fish in each length-category being a certain age. With fit this model with and without an $age\text{-}area$-interaction, and the former can be written as:

$$\log(CPUE_i) \sim \text{Student-}t(v, \mu_i, \sigma) \tag{10}$$

$$\mu_i = \beta_{0j[i]}(area_{ref}) + \beta_{1j[i]}(area_{heat}) + \beta_{2j[i]} age + \beta_{3j[i]}(age \times area_{heat}) \tag{11}$$

$$\begin{bmatrix} \beta_{0j} \\ \beta_{1j} \\ \beta_{2j} \\ \beta_{3j} \end{bmatrix} \sim \text{MVNormal}\left(\begin{bmatrix} \mu_{\beta_0} \\ \mu_{\beta_1} \\ \mu_{\beta_2} \\ \mu_{\beta_3} \end{bmatrix}, \begin{bmatrix} \sigma_{\beta_0} & 0 & 0 & 0 \\ 0 & \sigma_{\beta_1} & 0 & 0 \\ 0 & 0 & \sigma_{\beta_2} & 0 \\ 0 & 0 & 0 & \sigma_{\beta_3} \end{bmatrix} \right) \tag{12}$$

where β_{0j} and β_{1j} are the intercepts for the reference and heated areas, respectively, β_{2j} is the age slope for the reference area and β_{3j} is the interaction between age and $area$. All parameters vary by cohort (for cohort $j = 1981, \ldots, 2000$) and their correlation is set to 0 (Eq. 12). We use the following (vague) priors: $\mu_{\beta_{0,\ldots,3j}} \sim N(0, 10)$ (where μ_{β_2} is the population-level

estimate for $-Z_{ref}$ and $\mu_{\beta_2} + \mu_{\beta_3}$ is the population-level estimate for $-Z_{heat}$) and $v \sim gamma(2,0.1)$. σ and $\sigma_{\beta_{0,\ldots,3}}$ were given a $Student - t(3,0,2.5)$ prior.

Lastly, we quantified differences in the size-distributions between the areas using size-spectrum exponents. We estimate the biomass size-spectrum exponent γ directly, using the likelihood approach for binned data, i.e., the *MLEbin* method in the R package *sizeSpectra*(16, 47, 48). This method explicitly accounts for uncertainty in body masses *within* size-classes (bins) in the data and has been shown to be less biased than regression-based methods or the likelihood method based on bin-midpoints(16, 47). We pooled all years to ensure negative relationships between biomass and size in the size-classes (as the sign of the relationship varied between years).

All analyses were done using R(49) version 4.0.2 with R Studio (2021.09.1). The packages within the *tidyverse*(50) collection were used to processes and visualize data. Models where fit using the R package *brms*(51). When priors were not chosen based on the prior predictive distributions, we used the default priors from *brms* as written above. We used 3 chains and 4000 iterations in total per chain. Models were compared by evaluating their expected predictive accuracy (expected log pointwise predictive density) using leave-one-out cross-validation (LOO-CV)(52) while ensuring Pareto k values < 0.7, in the R package *loo*(53). Results of the model comparison can be found in the *Supporting Information*, Table S1-S4. We used *bayesplot*(54) and *tidybayes*(55) to process and visualize model diagnostics and posteriors. Model convergence and fit was assessed by ensuring potential scale reduction factors ($\hat{R}$) were less than 1.1, suggesting all three chains converged to a common distribution)(56), and by visually inspecting trace plots, residuals QQ-plots and with posterior predictive checks (*Supporting Information*, Fig. S2, S9, S11).

Results

Analysis of fish (perch) size-at-age using the von Bertalanffy growth equation (VBGE) revealed that fish cohorts (year classes) in the heated area both grew faster initially (larger size-at-age and VBGE K parameter) and reached larger predicted asymptotic sizes than those in the unheated reference area (Fig. 2). The model with area-specific VBGE parameters (L_∞, K and t_0) had best out of sample predictive accuracy (the largest expected log pointwise predictive density for a new observation; Table S1), and there is a clear difference in both the estimated values for fish asymptotic length (L_∞) and growth rate (K) between the heated and reference area (Fig. 2B-E). For instance, the distribution of differences between the heated and reference area of the posterior samples for L_∞ and K only had 11% and 2%, respectively, of the density below 0, illustrating that it is unlikely that the parameters are larger in the reference area or similar in the two areas (Fig. 2C, E). We estimated that the asymptotic length of fish in the heated area was 1.16 times larger than in the reference area ($L_{\infty\mathrm{heat}} = 45.7[36.8, 56.3]$, $L_{\infty\mathrm{ref}} = 39.4[35.4, 43.9]$, where the point estimate is the posterior median and values in brackets correspond to the 95% credible interval). The growth coefficient was 1.27 times larger in the heated area ($K_{\mathrm{heat}} = 0.19[0.15, 0.23], K_{\mathrm{ref}} = 0.15[0.12, 0.17]$). Also $t_{0\mathrm{heat}}$ was larger than $t_{0\mathrm{ref}}$ ($-0.16[-0.21, -0.11]$ vs $-0.44[-0.56, -0.33]$, respectively). These differences in growth parameters lead to fish being approximately 10% larger in the heated area relative to the reference area (Fig. S4).

In addition, we found that growth rates were both slower and declined faster with size compared to the heated area (Fig. 3). The best model for growth ($G = \alpha L^\theta$) had area-specific parameters (Table S2). Initial growth was estimated to be 1.18 times faster in the heated than in the reference area ($\alpha_{\mathrm{heat}} = 509.7[460.1,563.5]$, $\alpha_{\mathrm{ref}} = 433.5[413.3,454.1]$), and growth of fish in the heated area decline more slowly with length than in the reference area ($\theta_{\mathrm{heat}} = -1.13[-1.16, -1.11]$, $\theta_{\mathrm{ref}} = -1.18[-1.19, -1.16]$). The distribution of differences of the

295 posterior samples for α and θ both only had 0.3% of the density below 0 (Fig. 3C, E), indicating
296 high probability that growth rates have differentiated between the heated and reference area.
297 By analyzing the decline in catch-per-unit-effort over age, we found that the instantaneous
298 mortality rate Z (rate at which log abundance declines with age) is higher in the heated area
299 (Fig. 4). The overlap with zero is 0.05% for the distribution of differences of posterior samples
300 of Z_{heat} and Z_{ref} (Fig. 4C). We estimated Z_{heat} to be $0.7[0.67,0.82]$ and Z_{ref} to be
301 $0.63[0.57,0.68]$, which corresponds to annual mortality rates of 53% in the heated area and
302 47% in the reference area.
303 Lastly, analysis of the size-structure in the two areas revealed that, despite the faster growth
304 rates and larger sizes in the heated area for fish of all sizes, the higher mortality rates in the
305 heated area led to largely similar size-structures. Specifically, while largest fish were found in
306 the heated area, the size-spectrum exponent was only slightly larger in the heated area (Fig.
307 5A), and their 95% confidence intervals largely overlap (Fig. 5C).
308

309 ## Discussion

310 Our study provides strong evidence for warming-induced differentiation in growth, mortality,
311 and size-structure in a natural population of an unexploited, temperate fish species exposed to
312 an ecosystem-scale experiment with 5-10 ℃ above normal temperatures for more than two
313 decades. While it is a study on only a single species, these features make it a unique climate
314 change experiment, as experimental studies on fish to date are much shorter and often on scales
315 much smaller than whole ecosystems, and long time series of biological samples exist mainly
316 for commercially exploited fish species(30, 35, 57) (in which fisheries exploitation affects size-
317 structure both directly and indirectly by selecting for fast growing individuals). While factors
318 other than temperature could have contributed to the observed elevated growth and mortality,
319 the temperature contrast is unusually large for natural systems (i.e., 5-10 ℃, which can be

compared to the 1.35 ℃ change in the Baltic Sea between 1982 and 2006(58)). Moreover, heating occurred at the scale of a whole ecosystem, which makes the findings highly relevant in the context of global warming.

Interestingly, our findings contrast with both broader predictions about declining mean or adult body sizes based on the GOLT hypothesis(5, 59), and with intraspecific patterns such as the TSR (temperature-size rule(6)). The contrasts lie in that both asymptotic size and size-at-age of mature individuals, as well as the proportion of larger individuals were larger and higher in the heated area—despite the elevated mortality rates. This result was unexpected for two reasons: optimum growth temperatures generally decline with body size within species under food satiation in experimental studies(27), and fish tend to mature at smaller body size and allocate more energy into reproduction as it gets warmer(29). Both patterns have been used to explain how growth can increase for small and young fish, while large and old fish typically do not benefit from warming. Our study species is no exception to these rules(32, 60, 61). This suggests that growth dynamics under food satiation may not be directly proportional to those under natural feeding conditions(62). Moreover, our results suggest that growth changes emerge not only from direct physiological responses to increased temperatures, but also from warming-induced changes in the food web, e.g., prey productivity, diet composition and trophic transfer efficiencies(63). It also highlights that we need to focus on understanding to what extent the commonly observed increase in size-at-age for juveniles in warm environments can be maintained as they grow older.

Our finding that mortality rates were higher in the heated area was expected—warming leads to faster metabolic rates, which in turn is associated with shorter life span(11, 64, 65) (higher “physiological” mortality). Warming may also increase predation mortality, as predators’ feeding rates increase in order to meet the higher demand of food(12, 14, 23). However, most evidence to date of the temperature dependence of mortality rates in natural

populations stem from across species studies(12, 13, 66) (but see(23, 24)). Across species relationships are not necessarily determined by the same processes as within species relationships; thus, our finding of warming-induced mortality in a heated vs control environment in two nearby con-specific populations is important.

Since a key question for understanding the implications of warming on ectotherm populations is if larger individuals in a population become rarer or smaller(28, 67), within-species mortality responses to warming need further study. Importantly, this requires accounting also for effects of warming on growth, and how responses in growth and mortality depend on each other. For instance, higher mortality (predation or natural, physiological mortality) can release intra-specific competition and thus increase growth. Conversely, altered growth and body sizes can lead to changes in size-specific mortality, such as predation or starvation. In conclusion, individual-level patterns such as the TSR may be of limited use for predicting changes on the population-level size structure. This is because while warming increases growth for small fish, the effect on large fish is less consistent, and the TSR also does not account for changes in mortality or density dependence. Mortality may, however, be an important driver of the observed shrinking of ectotherms(68). Understanding the mechanisms by which the size- and age-distribution change with warming is critical for predicting how warming changes species functions and ecological roles(7, 63, 69). Our findings demonstrate that a key to do this is to acknowledge temperature effects on both growth and mortality and how they interact.

Acknowledgements

We thank all staff involved in data collection, and Jens Olsson and Göran Sundblad for discussion. This study was supported by SLU Quantitative Fish and Fisheries Ecology.

Code and Data Availability

All data and R code to reproduce the analyses can be downloaded from a GitHub repository (https://github.com/maxlindmark/warm_life_history) and will be archived on Zenodo upon publication. Researchers interested in using the data for purposes other than replicating our analyses are advised to request the data from the authors, as other useful information from the original data might not be included.

Author Contributions

ML conceived the idea and designed the study and the statistical analysis. Data-processing, initial statistical analyses, and initial writing was done by MK and ML. AG contributed critically to all mentioned parts of the paper. All authors contributed to the manuscript writing and gave final approval for publication.

References

1. E. O. Wilson, *The Diversity of Life* (Harvard University Press, 1992).

2. D. Atkinson, R. M. Sibly, Why are organisms usually bigger in colder environments? Making sense of a life history puzzle. *Trends in Ecology & Evolution* **12**, 235–239 (1997).

3. J. L. Gardner, A. Peters, M. R. Kearney, L. Joseph, R. Heinsohn, Declining body size: a third universal response to warming? *Trends in Ecology & Evolution* **26**, 285–291 (2011).

4. J. A. Sheridan, D. Bickford, Shrinking body size as an ecological response to climate change. *Nature Climate Change* **1**, 401–406 (2011).

5. W. W. L. Cheung, *et al.*, Shrinking of fishes exacerbates impacts of global ocean changes on marine ecosystems. *Nature Climate Change* **3**, 254–258 (2013).

6. D. Atkinson, Temperature and organism size—A biological law for ectotherms? *Advances in Ecological Research* **25**, 1–58 (1994).

7. K. J. Fritschie, J. D. Olden, Disentangling the influences of mean body size and size structure on ecosystem functioning: an example of nutrient recycling by a non-native crayfish. *Ecology and Evolution* **6**, 159–169 (2016).

8. G. Yvon-Durocher, J. M. Montoya, M. Trimmer, G. Woodward, Warming alters the size spectrum and shifts the distribution of biomass in freshwater ecosystems. *Global Change Biology* **17**, 1681–1694 (2011).

9. K. H. Andersen, Size-based theory for fisheries advice. *ICES J Mar Sci* **77**, 2445–2455 (2020).

10. J. L. Blanchard, R. F. Heneghan, J. D. Everett, R. Trebilco, A. J. Richardson, From bacteria to whales: Using functional size spectra to model marine ecosystems. *Trends in Ecology & Evolution* **32**, 174–186 (2017).

11. J. H. Brown, J. F. Gillooly, A. P. Allen, V. M. Savage, G. B. West, Toward a metabolic theory of ecology. *Ecology* **85**, 1771–1789 (2004).

12. D. Pauly, On the interrelationships between natural mortality, growth parameters, and mean environmental temperature in 175 fish stocks. *ICES Journal of Marine Science* **39**, 175–192 (1980).

13. J. T. Thorson, S. B. Munch, J. M. Cope, J. Gao, Predicting life history parameters for all fishes worldwide. *Ecological Applications* **27**, 2262–2276 (2017).

14. E. Ursin, A Mathematical Model of Some Aspects of Fish Growth, Respiration, and Mortality. *Journal of the Fisheries Research Board of Canada* **24**, 2355–2453 (1967).

15. J. R. Bernhardt, J. M. Sunday, P. L. Thompson, M. I. O'Connor, Nonlinear averaging of thermal experience predicts population growth rates in a thermally variable environment. *Proceedings of the Royal Society B: Biological Sciences* **285**, 20181076 (2018).

16. A. M. Edwards, J. P. W. Robinson, M. J. Plank, J. K. Baum, J. L. Blanchard, Testing and recommending methods for fitting size spectra to data. *Methods in Ecology and Evolution* **8**, 57–67 (2017).

17. R. W. Sheldon, W. H. Sutcliffe, A. Prakash, The Production of Particles in the Surface Waters of the Ocean with Particular Reference to the Sargasso Sea1. *Limnology and Oceanography* **18**, 719–733 (1973).

18. E. P. White, S. K. M. Ernest, A. J. Kerkhoff, B. J. Enquist, Relationships between body size and abundance in ecology. *Trends in Ecology & Evolution* **22**, 323–330 (2007).

19. R. F. Heneghan, I. A. Hatton, E. D. Galbraith, Climate change impacts on marine ecosystems through the lens of the size spectrum. *Emerging Topics in Life Sciences* **3**, 233–243 (2019).

20. K. H. Andersen, *Fish Ecology, Evolution, and Exploitation: A New Theoretical Synthesis* (Princeton University Press, 2019).

21. J. L. Blanchard, *et al.*, Do climate and fishing influence size-based indicators of Celtic Sea fish community structure? *ICES Journal of Marine Science* **62**, 405–411 (2005).

22. H. K. Barnett, T. P. Quinn, M. Bhuthimethee, J. R. Winton, Increased prespawning mortality threatens an integrated natural- and hatchery-origin sockeye salmon population in the Lake Washington Basin. *Fisheries Research* **227**, 105527 (2020).

23. P. A. Biro, J. R. Post, D. J. Booth, Mechanisms for climate-induced mortality of fish populations in whole-lake experiments. *Proceedings of the National Academy of Sciences* **104**, 9715–9719 (2007).

24. T. Berggren, U. Bergström, G. Sundblad, Ö. Östman, Warmer water increases early body growth of northern pike (Esox lucius) but mortality has larger impact on decreasing body sizes. *Can. J. Fish. Aquat. Sci.* (2021) https:/doi.org/10.1139/cjfas-2020-0386 (October 27, 2021).

25. L. A. K. Barnett, T. A. Branch, R. A. Ranasinghe, T. E. Essington, Old-Growth Fishes Become Scarce under Fishing. *Current Biology* **27**, 2843-2848.e2 (2017).

26. M. Daufresne, K. Lengfellner, U. Sommer, Global warming benefits the small in aquatic ecosystems. *Proceedings of the National Academy of Sciences, USA* **106**, 12788–12793 (2009).

27. M. Lindmark, J. Ohlberger, A. Gårdmark, Optimum growth temperature declines with body size within fish species. *Global Change Biology* **28**, 2259–2271 (2022).

28. J. Ohlberger, Climate warming and ectotherm body size – from individual physiology to community ecology. *Functional Ecology* **27**, 991–1001 (2013).

29. H. F. Wootton, J. R. Morrongiello, T. Schmitt, A. Audzijonyte, Smaller adult fish size in warmer water is not explained by elevated metabolism. *Ecology Letters* **n/a**.

30. R. E. Thresher, J. A. Koslow, A. K. Morison, D. C. Smith, Depth-mediated reversal of the effects of climate change on long-term growth rates of exploited marine fish. *Proceedings of the National Academy of Sciences, USA* **104**, 7461–7465 (2007).

31. A. Rindorf, H. Jensen, C. Schrum, Growth, temperature, and density relationships of North Sea cod (Gadus morhua). *Canadian Journal of Fisheries and Aquatic Sciences* **65**, 456–470 (2008).

32. M. Huss, M. Lindmark, P. Jacobson, R. M. van Dorst, A. Gårdmark, Experimental evidence of gradual size-dependent shifts in body size and growth of fish in response to warming. *Glob Change Biol* **25**, 2285–2295 (2019).

33. S. Smoliński, *et al.*, Century-long cod otolith biochronology reveals individual growth plasticity in response to temperature. *Sci Rep* **10**, 16708 (2020).

34. K. B. Oke, F. J. Mueter, M. A. Litzow, Warming leads to opposite patterns in weight-at-age for young versus old age classes of Bering Sea walleye pollock. *Can. J. Fish. Aquat. Sci.* (2022) https:/doi.org/10.1139/cjfas-2021-0315 (July 22, 2022).

35. A. R. Baudron, C. L. Needle, A. D. Rijnsdorp, C. T. Marshall, Warming temperatures and smaller body sizes: synchronous changes in growth of North Sea fishes. *Global Change Biology* **20**, 1023–1031 (2014).

36. D. R. Barneche, M. Jahn, F. Seebacher, Warming increases the cost of growth in a model vertebrate. *Functional Ecology* **33**, 1256–1266 (2019).

37. A. Audzijonyte, *et al.*, Trends and management implications of human-influenced life-history changes in marine ectotherms. *Fish and Fisheries* **17**, 1005–1028 (2016).

38. A. Adill, K. Mo, A. Sevastik, J. Olsson, L. Bergström, "Biologisk recipientkontroll vid Forsmarks kärnkraftverk (in Swedish)" (2013) (August 10, 2021).

39. M. Björklund, T. Aho, J. Behrmann-Godel, Isolation over 35 years in a heated biotest basin causes selection on MHC class IIß genes in the European perch (Perca fluviatilis L.). *Ecol Evol* **5**, 1440–1455 (2015).

40. J. R. Morrongiello, R. E. Thresher, A statistical framework to explore ontogenetic growth variation among individuals and populations: a marine fish example. *Ecological Monographs* **85**, 93–115 (2015).

41. T. E. Essington, M. E. Matta, B. A. Black, T. E. Helser, P. D. Spencer, Fitting growth models to otolith increments to reveal time-varying growth. *Can. J. Fish. Aquat. Sci.* **79**, 159–167 (2022).

42. G. Thoresson, "Metoder för övervakning av kustfiskbestånd (in Swedish)" (Kustlaboratoriet, Fiskeriverket, 1996) (September 28, 2021).

43. R. J. H. Beverton, S. J. Holt, *On the Dynamics of Exploited Fish Populations* (Fishery Investigations London Series 2, Volume 19., 1957).

44. L. von Bertalanffy, A quantitative theory of organic growth (inquiries on growth laws. II). *Human Biology* **10**, 181–213 (1938).

45. J. S. Wesner, J. P. F. Pomeranz, Choosing priors in Bayesian ecological models by simulating from the prior predictive distribution. *Ecosphere* **12**, e03739 (2021).

46. K. Lorenzen, Toward a new paradigm for growth modeling in fisheries stock assessments: Embracing plasticity and its consequences. *Fisheries Research* **180**, 4–22 (2016).

47. A. M. Edwards, J. P. W. Robinson, J. L. Blanchard, J. K. Baum, M. J. Plank, Accounting for the bin structure of data removes bias when fitting size spectra. *Marine Ecology Progress Series* **636**, 19–33 (2020).

48. A. Edwards, sizeSpectra: Fitting Size Spectra to Ecological Data Using Maximum Likelihood (2020).

49. R Core Team, *R: A Language and Environment for Statistical Computing. R Foundation for Statistical Computing* (2020).

50. H. Wickham, *et al.*, Welcome to the tidyverse. *Journal of Open Source Software*, 1686 (2019).

51. P.-C. Bürkner, **brms** : An *R* Package for Bayesian Multilevel Models Using *Stan*. *Journal of Statistical Software* **80** (2017).

52. A. Vehtari, A. Gelman, J. Gabry, Practical Bayesian model evaluation using leave-one-out cross-validation and WAIC. *Stat Comput* **27**, 1413–1432 (2017).

53. A. Vehtari, *et al.*, loo: Efficient leave-one-out cross-validation and WAIC for Bayesian models. (2020).

54. J. Gabry, D. Simpson, A. Vehtari, M. Betancourt, A. Gelman, Visualization in Bayesian workflow. *J. R. Stat. Soc. A* **182**, 389–402 (2019).

55. M. Kay, tidybayes: Tidy Data and Geoms for Bayesian Models (2019).

56. A. Gelman, J. Carlin, H. Stern, D. Rubin, *Bayesian Data Analysis. 2nd edition* (Chapman and Hall/CRC, 2003).

57. I. van Rijn, Y. Buba, J. DeLong, M. Kiflawi, J. Belmaker, Large but uneven reduction in fish size across species in relation to changing sea temperatures. *Global Change Biology* **23**, 3667–3674 (2017).

58. I. M. Belkin, Rapid warming of large marine ecosystems. *Progress in Oceanography* **81**, 207–213 (2009).

59. D. Pauly, The gill-oxygen limitation theory (GOLT) and its critics. *Science Advances* **7**, eabc6050 (2021).

60. P. Karås, G. Thoresson, An application of a bioenergetics model to Eurasian perch (Perca fluviatilis L.). *Journal of Fish Biology* **41**, 217–230 (1992).

61. O. Sandström, E. Neuman, G. Thoresson, Effects of temperature on life history variables in perch. *Journal of Fish Biology* **47**, 652–670 (1995).

62. S. F. Railsback, What We Don't Know About the Effects of Temperature on Salmonid Growth. *Transactions of the American Fisheries Society* **151**, 3–12 (2022).

63. A. Gårdmark, M. Huss, Individual variation and interactions explain food web responses to global warming. *Philosophical Transactions of the Royal Society B: Biological Sciences* **375**, 20190449 (2020).

64. M. W. McCoy, J. F. Gillooly, Predicting natural mortality rates of plants and animals. *Ecology Letters* **11**, 710–716 (2008).

65. S. B. Munch, S. Salinas, Latitudinal variation in lifespan within species is explained by the metabolic theory of ecology. *Proceedings of the National Academy of Sciences* **106**, 13860–13864 (2009).

66. H. Gislason, N. Daan, J. C. Rice, J. G. Pope, Size, growth, temperature and the natural mortality of marine fish: Natural mortality and size. *Fish and Fisheries* **11**, 149–158 (2010).

67. J. Ohlberger, E. J. Ward, D. E. Schindler, B. Lewis, Demographic changes in Chinook salmon across the Northeast Pacific Ocean. *Fish and Fisheries* **19**, 533–546 (2018).

68. I. Peralta-Maraver, E. L. Rezende, Heat tolerance in ectotherms scales predictably with body size. *Nat. Clim. Chang.* **11**, 58–63 (2021).

69. A. Audzijonyte, *et al.*, Fish body sizes change with temperature but not all species shrink with warming. *Nat Ecol Evol* **4**, 809–814 (2020).

553 Figures

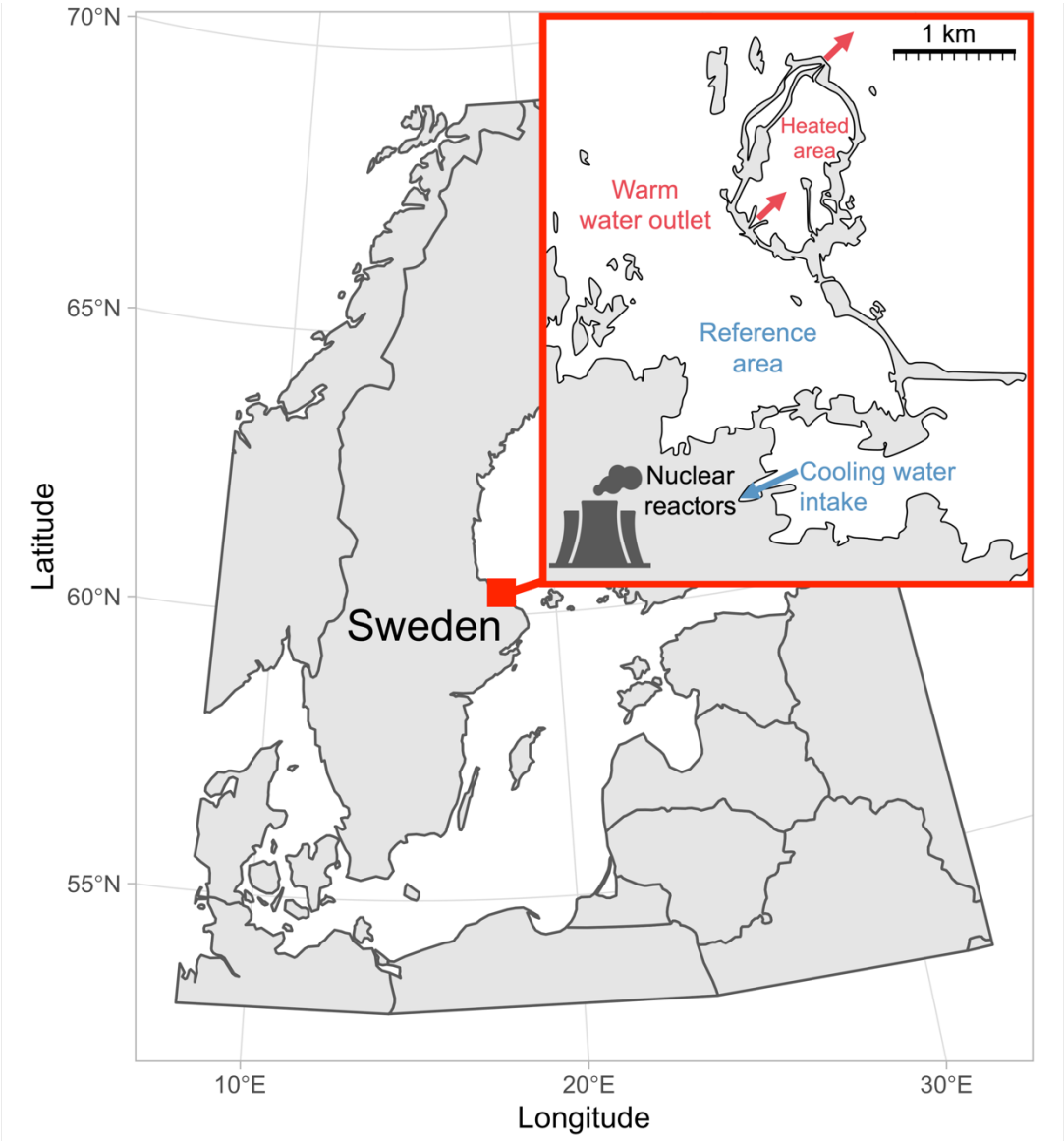

554

555 **Fig. 1.** Map of the area with the unique whole-ecosystem warming experiment from which
556 perch in this study was sampled. Inset shows the 1 km^2 enclosed coastal bay that has been
557 artificially heated for 23 years, the adjacent reference area with natural temperatures, and
558 locations of the cooling water intake and where the heated water outlet from nuclear power
559 plants enters the heated coastal basin.

560

561

562

563

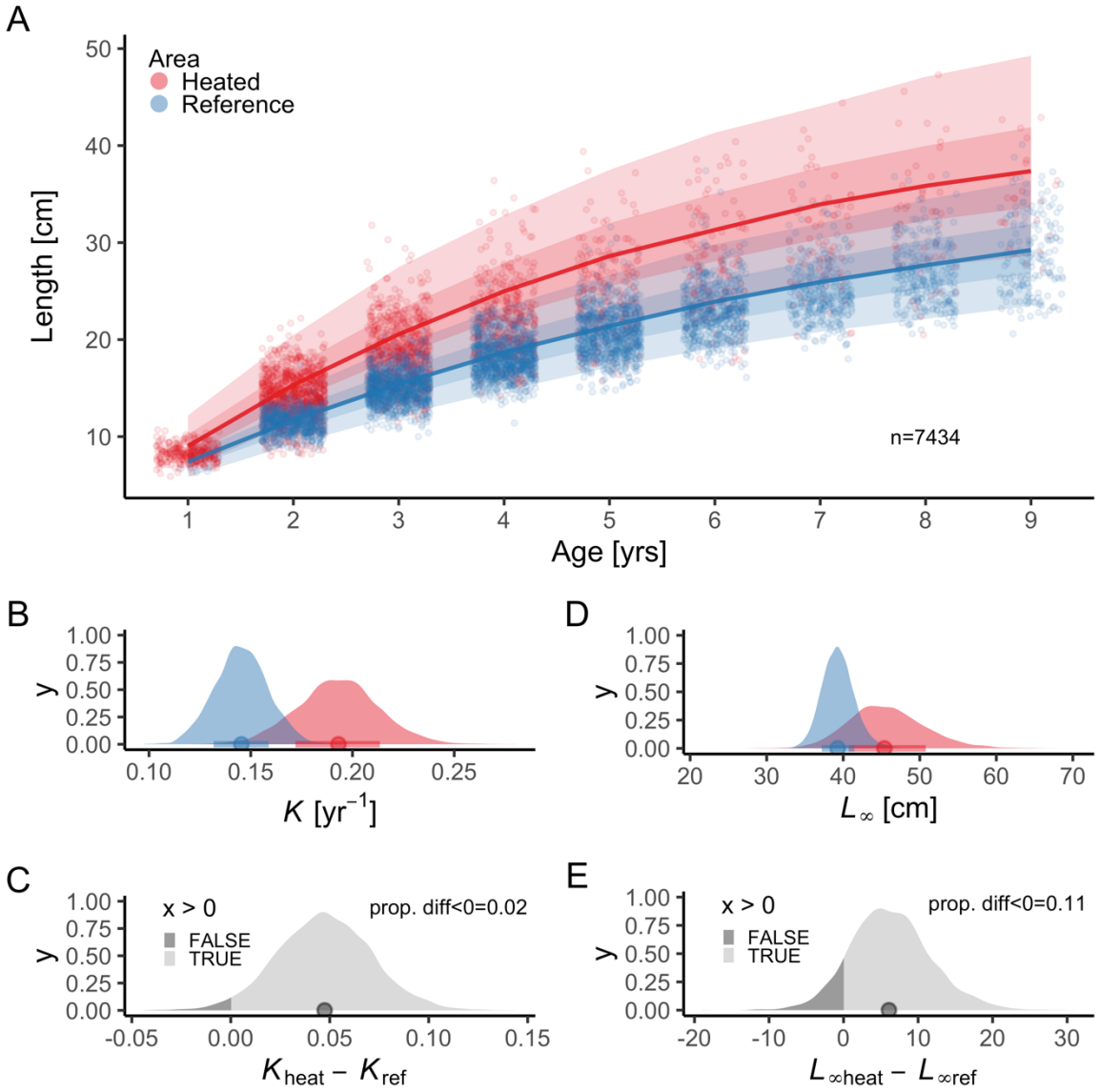

564

565 **Fig. 2.** Fish grow faster and reach larger sizes in the heated (red) enclosed bay compared to the
566 reference (blue) area. Points in panel (A) depict individual-level length-at-age and lines show
567 the global posterior prediction (both exponentiated) without group-level effects (i.e., cohort)
568 from the von Bertalanffy growth model with area-specific coefficients. The shaded areas
569 correspond to 50% and 90% credible intervals. Panel (B) shows the posterior distributions for
570 growth coefficient (parameters K_{heat} (red) and K_{ref} (blue)) and (C) the distribution of their
571 difference. Panel (D) shows the posterior distributions for asymptotic length (parameters
572 $L_{\infty\text{heat}}$ and $L_{\infty\text{ref}}$), and (E) the distribution of their difference.

573

574

575

576

577

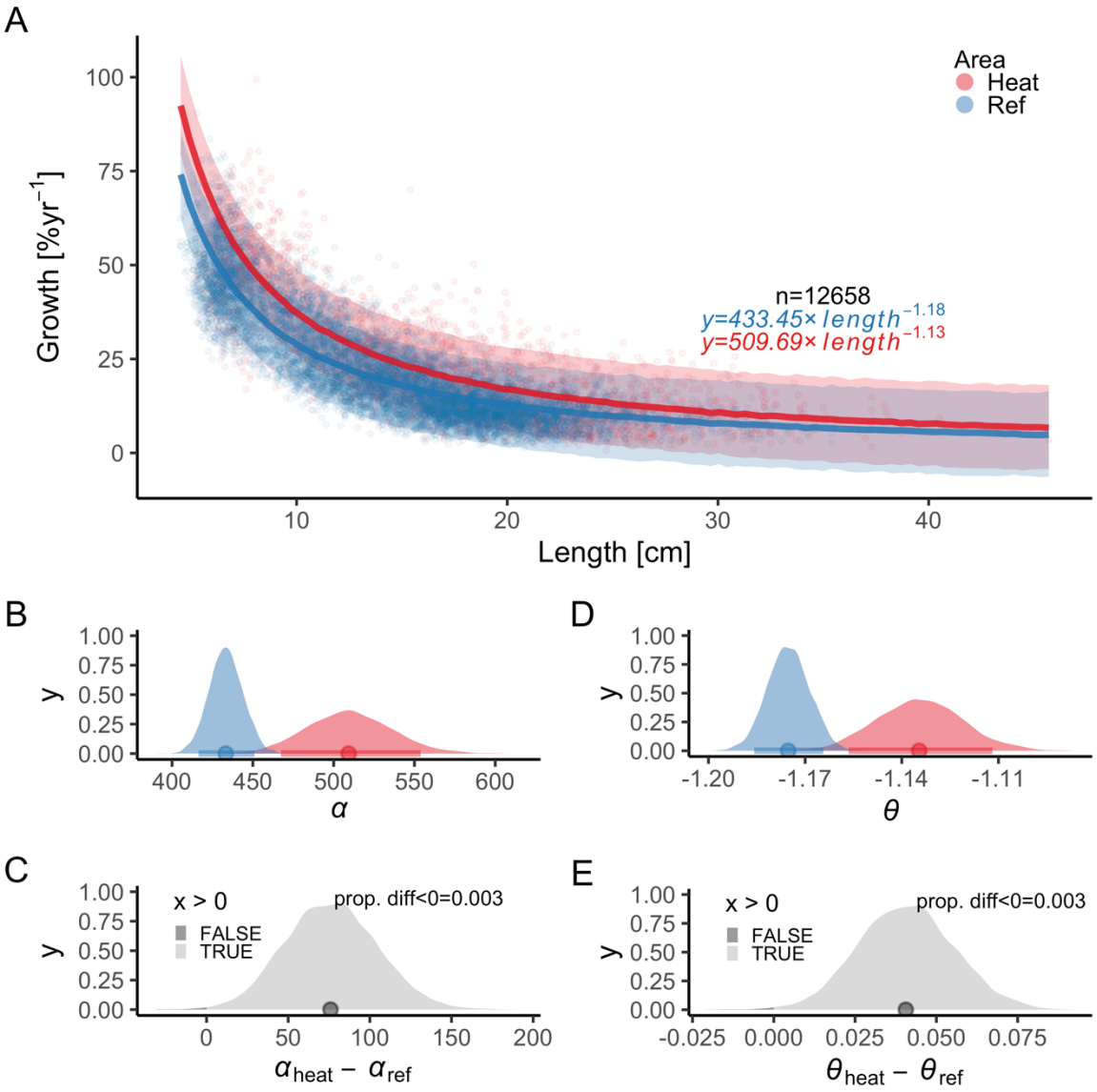

578

579 **Fig. 3.** The faster growth rates in the heated area (red) compared to the reference (blue) are
580 maintained as fish grow. The points illustrate specific growth estimated from back-calculated
581 length-at-age (within individuals) as a function of length (expressed as the geometric mean of
582 the length at the start and end of the time interval). Lines show the global posterior prediction
583 without group-level effects (i.e., individual within cohort) from the allometric growth model
584 with area-specific coefficients. The shaded areas correspond to the 90% credible interval. The
585 equation uses mean parameter estimates. Panel (B) shows the posterior distributions for initial
586 growth (α_{heat} (red) and α_{ref} (blue)), and (C) the distribution of their difference. Panel (D)
587 shows the posterior distributions for the allometric decline in growth with length (θ_{heat} and
588 θ_{ref}), and (E) the distribution of their difference.

589

590

591

592

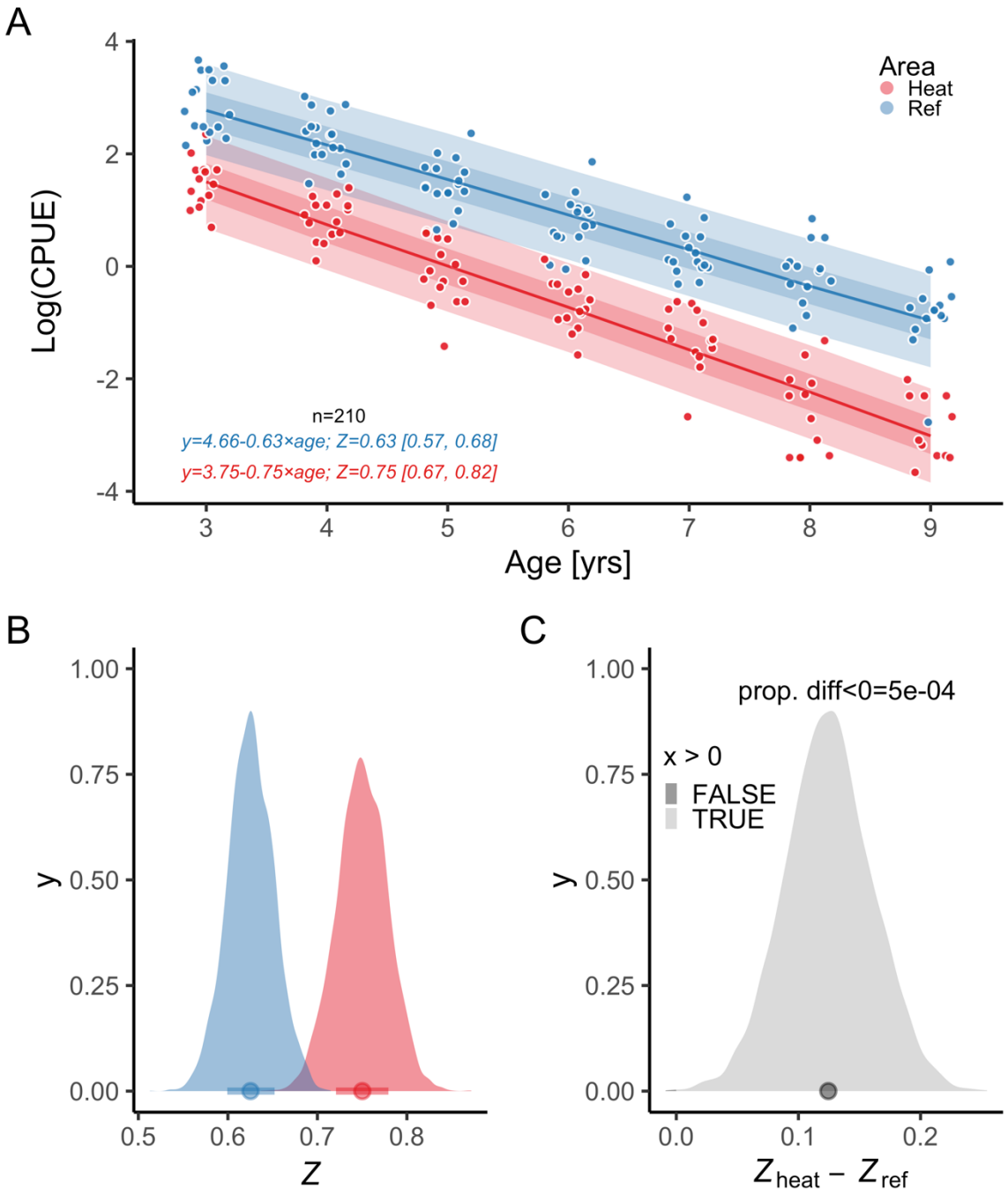

593

594 **Fig. 4.** The instantaneous mortality rate (Z) is higher in the heated area (red) than in the
595 reference (blue). Panel (A) shows the $log\ (CPUE)$ as a function of age, where the slope
596 corresponds to the global $-Z$. Lines show the posterior prediction without group-level effects
597 (i.e., cohort) and the shaded areas correspond to the 50% and 90% credible intervals. The
598 equation uses mean parameter estimates. Panel (B) shows the posterior distributions for
599 mortality rate (Z_{heat} and Z_{ref}), and (C) the distribution of their difference.

600

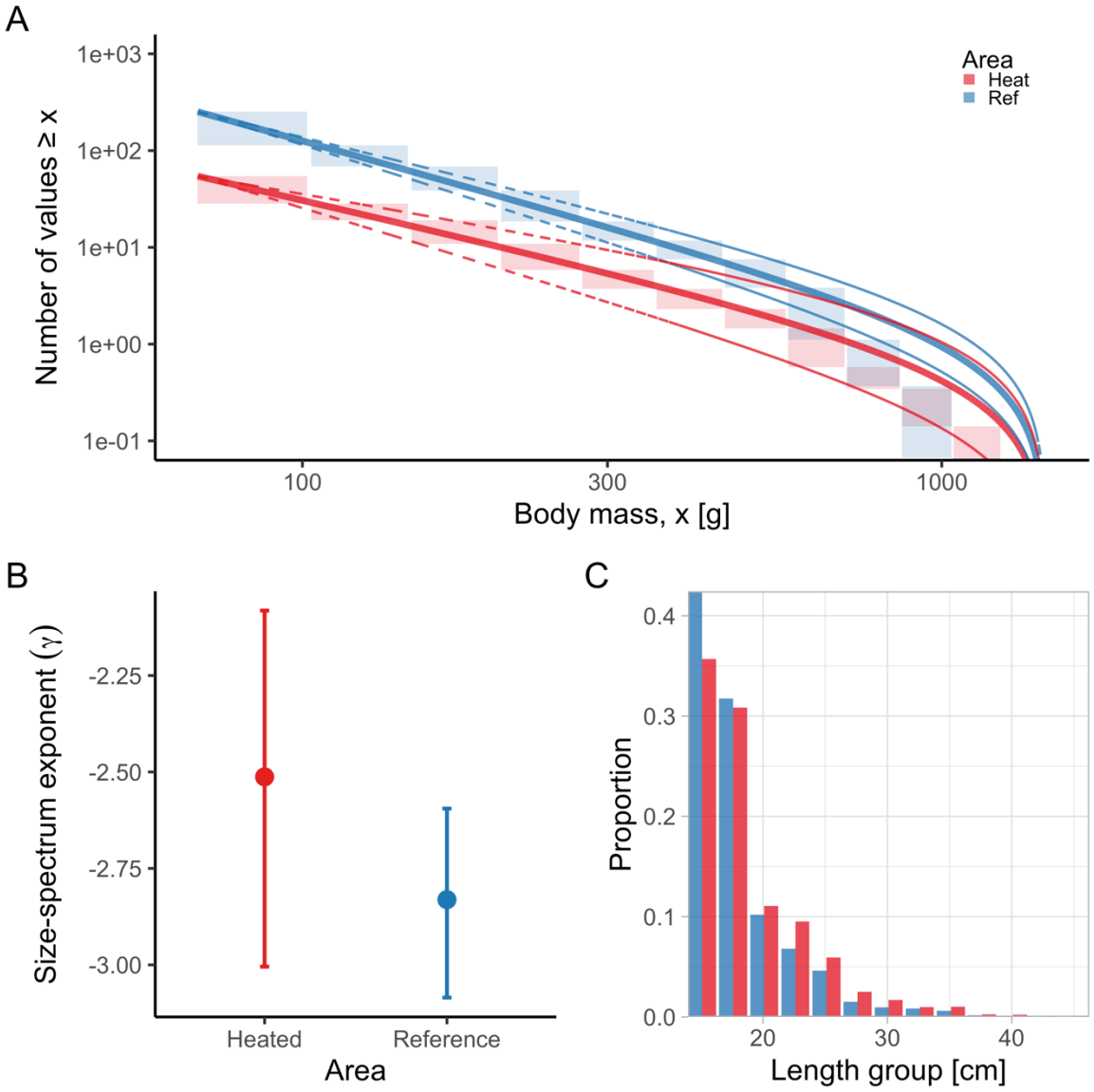

Fig. 5. The heated area (red) has a larger proportion of large fish than the reference area (blue), illustrated both in terms of the biomass size-spectrum (A), and histograms of proportions (C), but the difference in the slope of the size-spectra between the areas is not statistically clear (B). Panel (A) shows the size distribution and MLEbins fit (red and blue solid curve for the heated and reference area, respectively) with 95% confidence intervals indicated by dashed lines. The vertical span of rectangles illustrates the possible range of the number of individuals with body mass ≥ the body mass of individuals in that bin. Panel (B) shows the estimate of the size-spectrum exponent, γ, and vertical lines depict the 95% confidence interval. Panel (C) illustrates histograms of length groups in the heated and reference area as proportions (for all years pooled).